NASA/TM—2017-219536

Experimental Investigation of Shrouding on Meshed Spur Gear Windage Power Loss

Irebert R. Delgado
Glenn Research Center, Cleveland, Ohio

Michael J. Hurrell
HX5 Sierra LLC, Cleveland, Ohio

September 2017

NASA STI Program . . . in Profile

Since its founding, NASA has been dedicated to the advancement of aeronautics and space science. The NASA Scientific and Technical Information (STI) Program plays a key part in helping NASA maintain this important role.

The NASA STI Program operates under the auspices of the Agency Chief Information Officer. It collects, organizes, provides for archiving, and disseminates NASA's STI. The NASA STI Program provides access to the NASA Technical Report Server—Registered (NTRS Reg) and NASA Technical Report Server—Public (NTRS) thus providing one of the largest collections of aeronautical and space science STI in the world. Results are published in both non-NASA channels and by NASA in the NASA STI Report Series, which includes the following report types:

- TECHNICAL PUBLICATION. Reports of completed research or a major significant phase of research that present the results of NASA programs and include extensive data or theoretical analysis. Includes compilations of significant scientific and technical data and information deemed to be of continuing reference value. NASA counter-part of peer-reviewed formal professional papers, but has less stringent limitations on manuscript length and extent of graphic presentations.

- TECHNICAL MEMORANDUM. Scientific and technical findings that are preliminary or of specialized interest, e.g., "quick-release" reports, working papers, and bibliographies that contain minimal annotation. Does not contain extensive analysis.

- CONTRACTOR REPORT. Scientific and technical findings by NASA-sponsored contractors and grantees.

- CONFERENCE PUBLICATION. Collected papers from scientific and technical conferences, symposia, seminars, or other meetings sponsored or co-sponsored by NASA.

- SPECIAL PUBLICATION. Scientific, technical, or historical information from NASA programs, projects, and missions, often concerned with subjects having substantial public interest.

- TECHNICAL TRANSLATION. English-language translations of foreign scientific and technical material pertinent to NASA's mission.

For more information about the NASA STI program, see the following:

- Access the NASA STI program home page at http://www.sti.nasa.gov

- E-mail your question to help@sti.nasa.gov

- Fax your question to the NASA STI Information Desk at 757-864-6500

- Telephone the NASA STI Information Desk at 757-864-9658

- Write to:
  NASA STI Program
  Mail Stop 148
  NASA Langley Research Center
  Hampton, VA 23681-2199

NASA/TM—2017-219536

Experimental Investigation of Shrouding on Meshed Spur Gear Windage Power Loss

Irebert R. Delgado
Glenn Research Center, Cleveland, Ohio

Michael J. Hurrell
HX5 Sierra LLC, Cleveland, Ohio

Prepared for the
73rd Annual Forum and Technology Display (Forum 73)
sponsored by the American Helicopter Society (AHS)
Fort Worth, Texas, May 9–11, 2017

National Aeronautics and
Space Administration

Glenn Research Center
Cleveland, Ohio 44135

September 2017

Acknowledgments

The authors acknowledge the support of the NASA Revolutionary Vertical Lift Technology Project and the technical test support provided by Sigurds Lauge (HX5 Sierra LLC).

This work was sponsored by the Advanced Air Vehicle Program at the NASA Glenn Research Center.

Level of Review: This material has been technically reviewed by technical management.

Available from

NASA STI Program
Mail Stop 148
NASA Langley Research Center
Hampton, VA 23681-2199

National Technical Information Service
5285 Port Royal Road
Springfield, VA 22161
703-605-6000

This report is available in electronic form at http://www.sti.nasa.gov/ and http://ntrs.nasa.gov/

Experimental Investigation of Shrouding on Meshed Spur Gear Windage Power Loss

Irebert R. Delgado
National Aeronautics and Space Administration
Glenn Research Center
Cleveland, Ohio 44135

Michael J. Hurrell
HX5 Sierra LLC
Cleveland, Ohio 44135

Summary

Windage power loss in high-speed gearboxes results in efficiency losses and increased heating due to drag on the gear teeth. Test results for meshed spur gear windage power loss are presented at ambient oil inlet temperatures, both with and without shrouding. The rate of windage power loss is observed to increase above a gear surface speed of 10,000 ft/min (51 m/s), similar to results presented in the literature. Shrouding is observed to become more effective above 15,000 ft/min (76 m/s), decreasing power loss by 10 percent at 25,000 ft/min (127 m/s). The need for gearbox oil drain slots limits the effectiveness of shrouding in reducing windage power loss. Windage power loss is observed to decrease with increasing gearbox temperatures and to increase with oil flow. Windage power losses for unshrouded meshed spur gears are 7 times greater than losses determined from unshrouded single spur gear tests. A 6- to 12-times increase in windage power loss is observed in the shrouded meshed spur gear data compared with shrouded single spur gear data. Based on this preliminary study, additional research is suggested to determine the effect of oil drain slot configurations, axial and radial shroud clearances, and higher gear surface speeds on windage power loss. Additional work is also suggested to determine the sensitivity of windage power loss to oil temperature and oil flow. Windage power loss for meshed spur gears tested in both the shrouded and unshrouded configurations is shown to be more than double versus windage power loss for the same spur gears run individually in the same shroud configurations. Further study of the physical processes behind these results is needed to optimize gearbox shrouds for minimum windage power loss.

Introduction

With an increasing demand for air transport and fuel, NASA aeronautics research is addressing the need for more efficient and flexible air transportation. An area of focus is in developing, maturing, and demonstrating rotorcraft drive system technologies “to enable increased vehicle speeds while maximizing propulsive efficiency and minimizing weight penalties” (Ref. 1). Rotorcraft gearboxes with efficiencies of 95 percent or more still incur windage power losses at high gear speeds. In general, experience has shown that high-speed effects become significant at pitch-line velocities greater than 10,000 ft/min (51 m/s), as noted in Dudley (Ref. 2). Eastwick and Johnson (Ref. 3) define windage power loss as power loss “due to the fluid drag experienced by the gear when it is running in air or in an air-oil mist.” This phenomena results in inefficiencies in the gear or gear system in transmitting load, resulting in power loss. For a rotorcraft drive system, more torque is then necessary at the gearbox input to provide an equivalent power

output to the rotor blades. Even small percent reductions in available torque can reduce performance factors such as mission payload, maximum hover ceiling, and rate of climb (Ref. 4).

Shrouding is one method of reducing windage power loss. Single-gear experiments in air by Dawson (Ref. 5) using a 1.1-in. (27-mm) axial shroud clearance and a 0.6-in. (15-mm) radial shroud clearance encompassing 270° around the gear showed a decrease in power loss of nearly 50 percent. In tests of single spur gears in air and oil, Handschuh and Hurrell (Ref. 6) found that the minimum axial and radial shroud clearance tests resulted in the lowest observed windage power loss. Hill et al. (Ref. 7) developed a computational fluid dynamics method to study gear windage aerodynamics to analyze the effect of shrouding on spur gear experiments performed by Diab et al. (Ref. 8) and found an 81 percent decrease in power loss at 8100 rpm (850 rad/s) with a radial and axial clearance of 0.026 in. (0.66 mm). Finally, Winfree (Ref. 9) experimentally showed a decrease in gear windage power loss through the use of baffling on a single bevel gear with water as a lubricant.

Analytically, for a single spur gear, Hill et al. (Ref. 7) showed flow entering axially into the space between gear teeth, impinging on the leading tooth edge and then being ejected radially outward. This is generally in agreement with experimental findings by Dawson (Ref. 5), who conducted visualization studies using smoke. This impingement of the air and oil fluid flow on the gear teeth is largely responsible for the windage power loss. Further, Hill et al. showed that the use of close-clearance shrouding results in the fluid flow generally remaining at the tangential velocities found at the gear surface, thus conserving fluid angular momentum. This results in a decreased power loss.

A number of experiments by Lord (Ref. 10) studied the effect of shrouding on power loss for both single and meshed spur gears as well as the influence of tooth geometry and lubricant flow. This paper details preliminary shrouded meshed spur gear experimental work conducted at NASA Glenn Research Center's windage rig facility. The meshed spur gear windage power loss data will be compared with available experimental data and analyses. The data is specific to the Glenn windage rig and will be used as a baseline for further tests to investigate shrouding effects, oil temperature, oil flow, and gear geometry modifications that could mitigate windage power loss. This paper will do the following:

(1) Compare windage power loss data for meshed spur gears with existing experimental and analytical data for single spur gears.

(2) Compare windage power loss data for meshed spur gears in an unshrouded versus shrouded configuration.

(3) Outline additional research given the experimental data and analysis and existing literature.

Experimental

The windage power loss test rig is described, and details are given on the test gears, shroud configurations, and experimental procedure. Finally, the windage power loss calculation is provided.

Test Rig

Power loss data were collected in Glenn's gear windage research facility (Figure 1). The input shaft of the test gearbox is connected to the 150 hp (112 kW) dc drive motor and 5.17:1 speedup gearbox. An opposing torque can be applied on the test gearbox output shaft using an eddy current dynamometer rated to 890 in·lb (100 N·m) at 2865 rpm (300 rad/s). Clutches located forward of the torque meter and dynamometer allow for disengagement of the test gearbox input and output shafts. This enables the test hardware (e.g., shafts, bearings, and test gears) to coast down from a preset pitch-line velocity. Current tests were limited to approximately 28,000 ft/min (142 m/s).

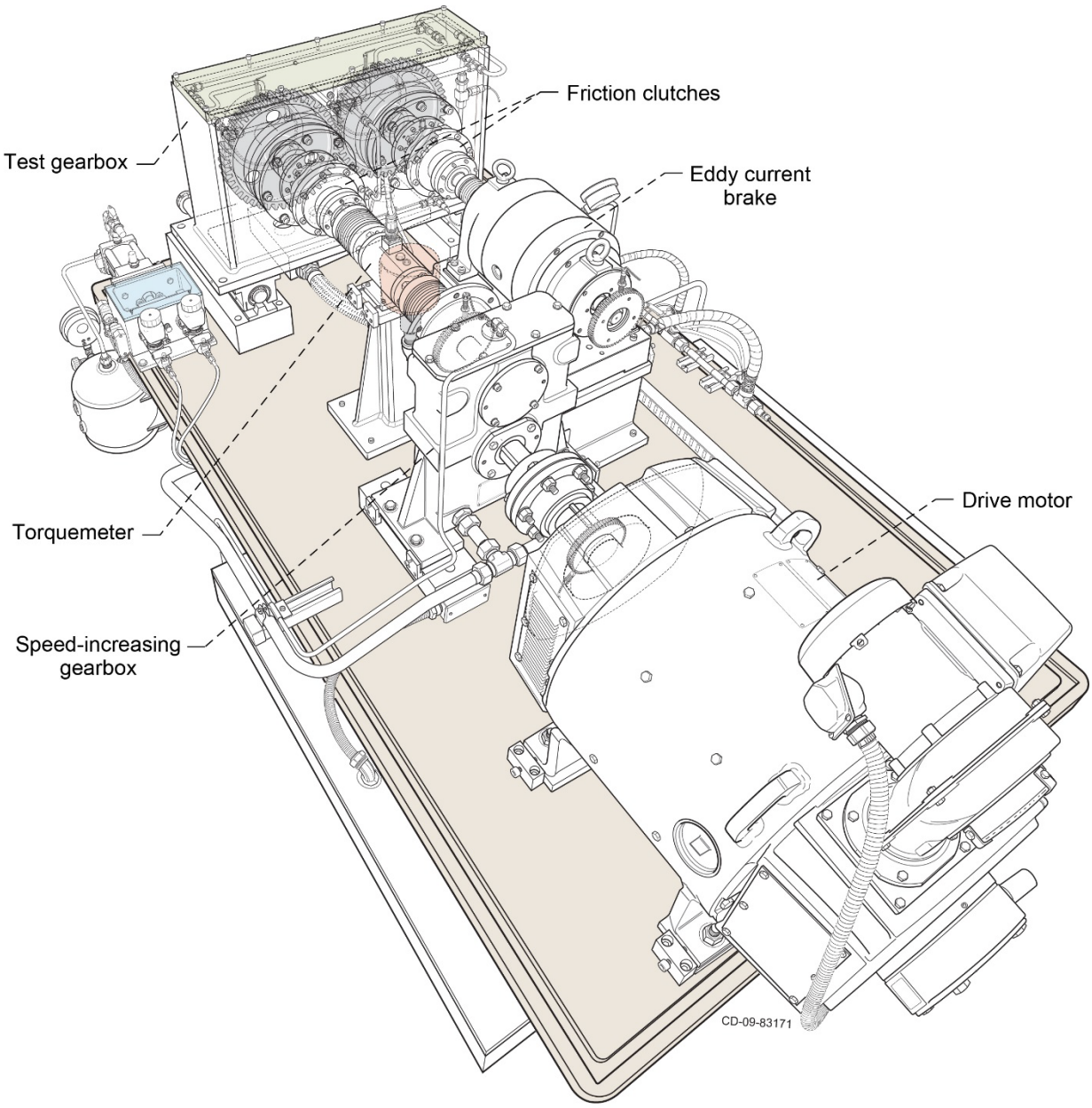

Figure 1.—NASA Glenn Research Center gear windage test rig.

Tests can be run with and without shrouding. Aluminum plates (6061-T6) are used for the axial shrouds, and A366 low-carbon steel 0.063-in. (1.6-mm) sheet metal strips are used for radial shrouding (Figure 2). The shrouds are placed within a clamshell housing (Figure 3). The lower halves of both the drive- and driven-side clamshell housing contain four oil drain holes each, 0.75 in. wide by 3.5 in. long (19 by 89 mm). The shroud surface roughness is approximately 63 μin (1.6 μm). Six machined slots within the clamshell housing allow for set clearances between the axial shroud wall and gear. The axial shroud walls, in turn, have six machined slots to vary the radial shroud position (Figure 2 and Figure 3). For ease of assembly, the clamshell housing is composed of four pieces: (1) upper drive side, (2) lower drive side, (3) upper driven side, and (4) lower driven side. The entire assembly is mounted within the test gearbox enclosing the test gears (Figure 1 and Figure 4).

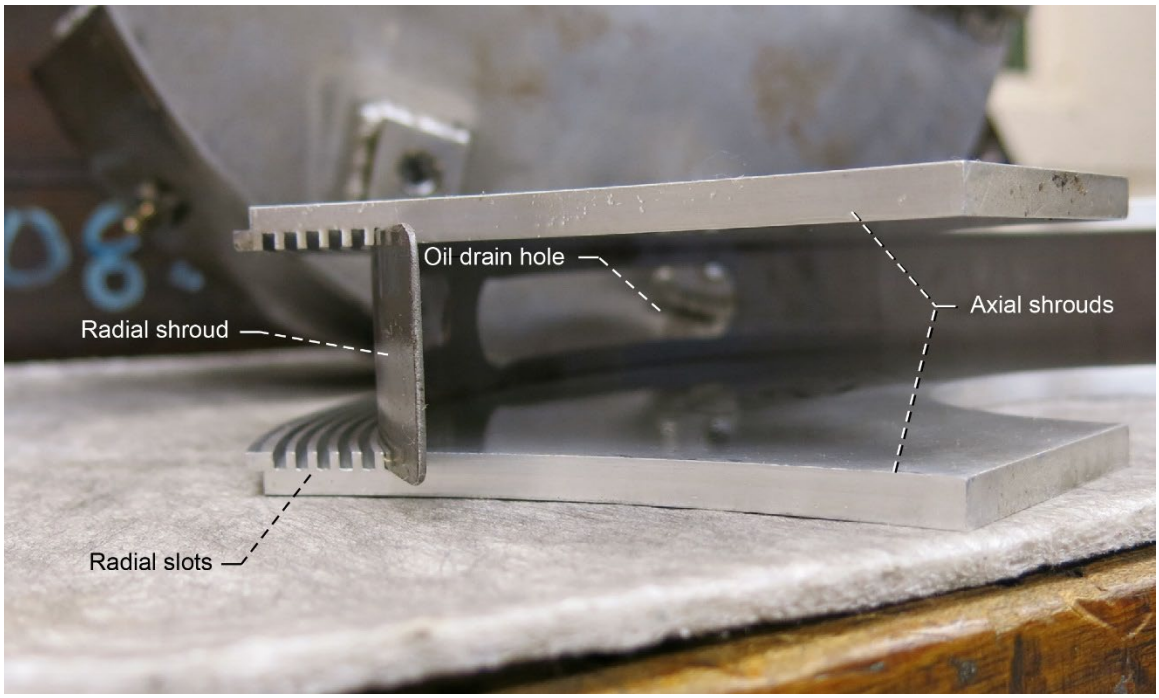

Figure 2.—Closeup of 0.04-in. (1.00-mm) axial and radial clearance shrouding.

Figure 3.—Quarter section of clamshell housing (drive side, upper half) locating axial and radial shrouds.

The test gearbox can accommodate both single or meshed spur and helical gear designs. The test gearbox interior dimensions are approximately 6 in. wide by 16 in. deep by 28 in. high (150 by 410 by 710 mm). Speed wheels consisting of 60 toothed wheels are mounted on the rig shafting. For each speed wheel, a variable reluctance magnetic speed sensor is bracket-mounted to the rig frame to measure shaft speed. Six speed wheel and magnetic speed pickup pairs are located at the drive motor, speedup gearbox,

input shaft, output shaft, and dynamometer. Accelerometers are located at the speedup gearbox, torque meter, test rig, and dynamometer. Thermocouples are located at the oil inlet and the oil exit, at four bearing locations on the test rig, and at a location just out-of-mesh of the test gears but within the clamshell housing. Gear fling-off temperature is measured at the 1 o'clock position on the drive-side test gear. Torque is measured with a rotary torque sensor rated at 2000 in·lb (230 N·m) and located inline between the speedup gearbox and test rig. For safety, a large containment shield is rolled into place over the test rig prior to operation (Figure 5).

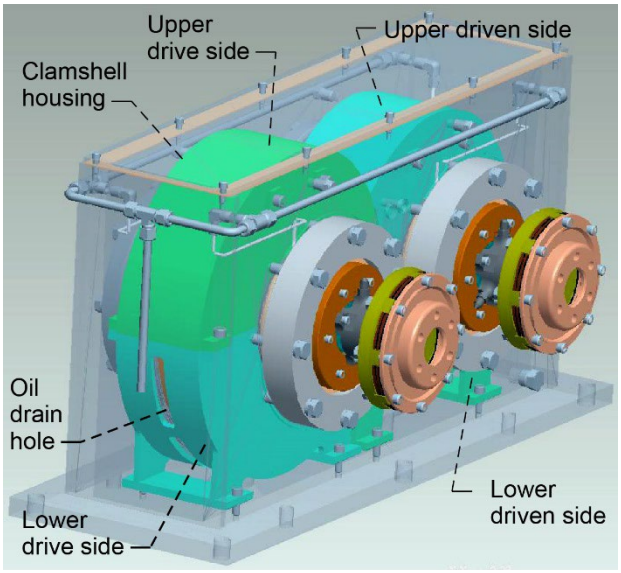

Figure 4.—Test gearbox with axial and radial shrouds in clamshell housing.

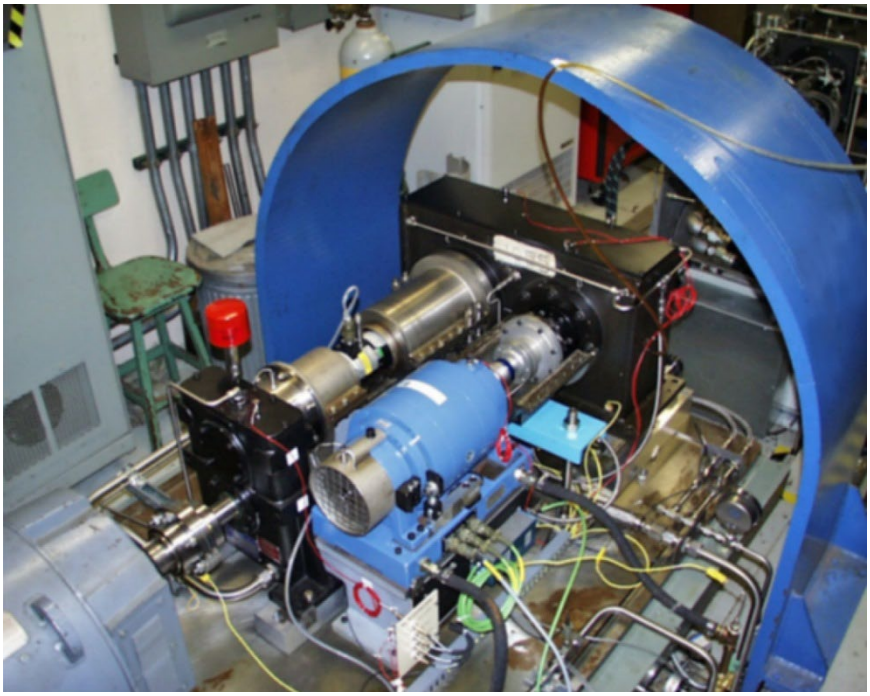

Figure 5.—Containment shield over test gearbox.

Experiment

Table I gives basic gear information on the meshed spur gears to be tested. An opposing torque of 10 in·lb (1.1 N·m) was applied with the dynamometer to lightly load the meshed gears to prevent backside contact and excessive vibration due to gear rattle. The gears were tested at three different sets of axial and circumferential clearances: unshrouded (U), clamshell (CS), and shrouded 0.04-in. (1.0-mm) axial and radial clearance (C1). Nominal axial and circumferential dimensions are given in Table II. Figure 6 shows the 0.04-in. axial and radial shrouding configuration prior to assembly. Tests were conducted at ambient air and oil inlet temperatures. The meshed spur gears were spun in the direction shown in Figure 7 to 10,000 rpm (1047 rad/s) in 2000 rpm (209 rad/s) increments. The clutches were then energized to disengage both the drive motor and the dynamometer from the test gears and the input and output shafts. The system was allowed to coast or wind down to a surface velocity of zero. This process was repeated two additional times. Data was recorded in LabVIEW (National Instruments Corporation) at a 3-Hz capture rate. To prevent churning, the radial shrouds have an oil drain hole at the 6 o'clock position (Figure 2 and Figure 6).

TABLE I.—BASIC MESHED SPUR GEAR INFORMATION

Gear parameter	Drive side	Driven side
Number of teeth	44	52
Diametral pitch, P_d, 1/in. (module (M), mm)	4 (6.35)	
Face width, in. (mm)	1.1 (28.5)	1.1 (28.5)
Pitch diameter, in. (mm)	11.0 (279.4)	13.0 (330.2)
Pressure angle, deg (rad)	25 (0.44)	
Outside diameter, in. (mm)	11.5 (291.9)	13.5 (342.7)
Material	Steel—SAE 5150H	

TABLE II.—SHROUD CONFIGURATION CLEARANCES

Shroud configuration	Axial clearance	Radial clearance	
	Per side, in. (mm)	Drive side, in. (mm)	Driven side, in. (mm)
(U) Unshrouded	2.3 (57.2)	2.5 (63.5)	1.0 (25.4)
(CS) Clamshell housing	1.5 (38.1)	0.8 (20.8)	0.8 (20.8)
(C1) Shrouded	0.04 (1.0)	0.04 (1.0)	0.04 (1.0)

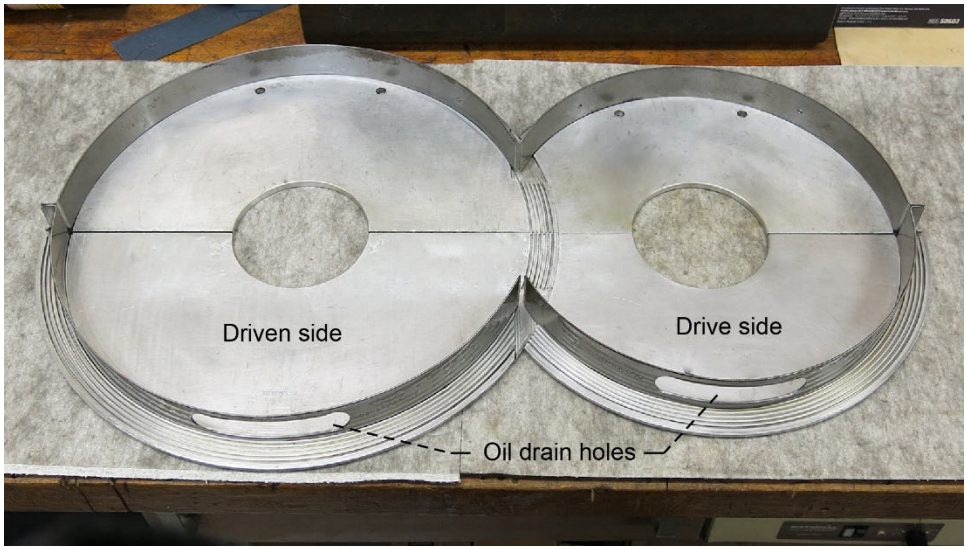

Figure 6.—C1 shroud configuration (0.04-in. (1.00-mm) axial and radial clearance) with drain holes.

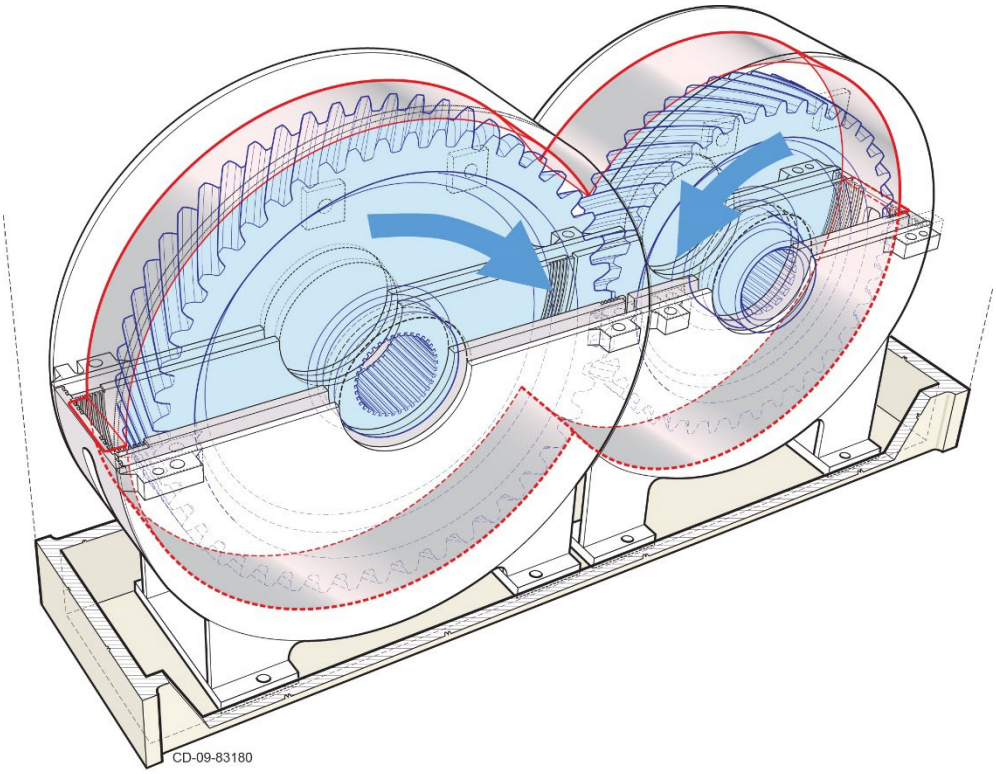

Figure 7.—Meshed gears within clamshell housing and shrouding; arrows show direction of rotation.

Power Loss Calculation

Total power loss consists of gear mesh losses, rig driveline losses, and windage losses. Considering the light loading of the gear set during the tests reported herein, the gear mesh losses are minimal: 0.13 hp (0.097 kW) at 10 in·lb (1.13 N·m) torque, conservatively calculated based on an analytical method by Anderson and Loewenthal (Ref. 11). The rig driveline losses, or tare losses, consist of power losses associated with the spinning drive shaft, driven shaft, and support bearings. These losses are determined by performing spin-down tests without the test gears installed.

Similar to the Dawson study (Ref. 5), power loss due to windage is calculated, in part, by plotting the angular velocity versus time curve during free deceleration and measuring the slope or instantaneous angular acceleration at various points on that curve. Torque is given by the product of the angular acceleration and the moment of inertia. An equivalent moment of inertia, J_{eq}, for the meshed gear system is given by Equation (1) (Ref. 12). The windage power loss of the meshed-gear system is calculated from the product of the torque and the shaft speed. Finally, the windage power loss attributable to the gears alone is determined by subtracting the tare power loss from the total system power loss.

$$J_{eq} = J_1 + J_2\left(\frac{N_1}{N_2}\right)^2 \tag{1}$$

where

J_1 moment of inertia of the pinion
J_2 moment of inertia of the gear
N_1 number of pinion teeth
N_2 number of gear teeth

Component inertias were measured using the curved rail method and calculated as outlined by Genta and Delprete (Eq. (2), Ref. 12). Figure 8 shows the experimental setup for the curved rail procedure. The test shaft assemblies, drive and driven, were assembled with and without the test gears. The inertias measured using the test shaft assemblies without the test gears were used in calculating the rig driveline losses. The inertias measured using the test shaft assemblies with the test gears were used in determining the gear windage power losses.

$$J = mr^2\left[\frac{gT^2}{4\pi(R-r)} - 1\right] \tag{2}$$

where

J moment of inertia of the assembly
m total mass of the assembly
r radius of shaft-bearing journal
R radius of curved rail of test apparatus
T period of oscillation of assembly
g gravitational constant

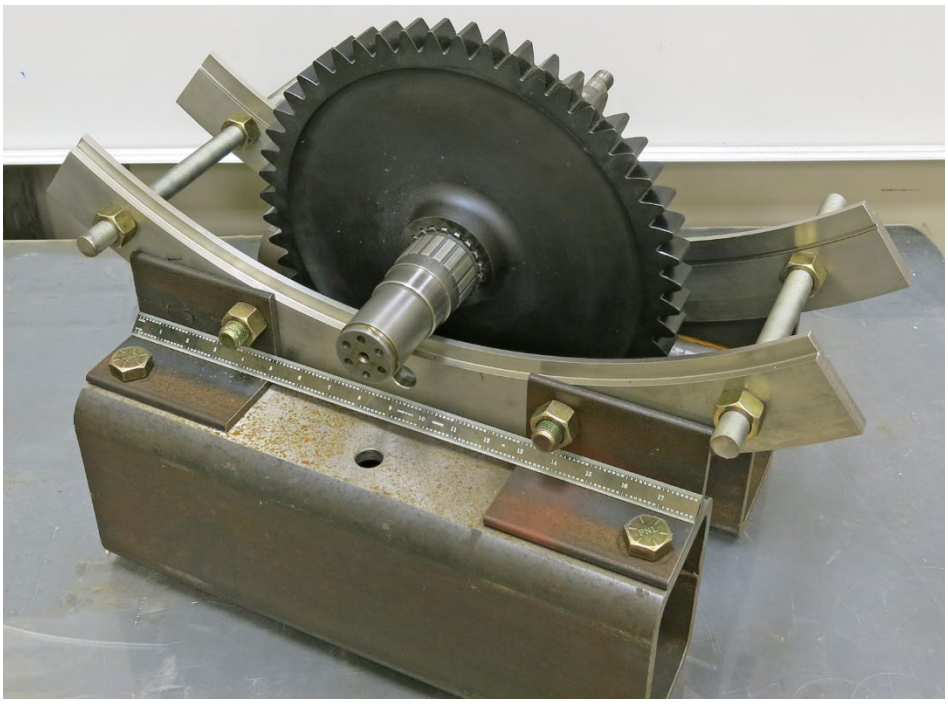

Figure 8.—Experimental setup using curved rail method to calculate tare loss (in part) (Ref. 11).

Results and Discussion

Figure 9 shows very repeatable data for windage power loss tests of meshed spur gears on three successive test days. Data is shown for wind-down cycle 3 for each test day. For the C1 shroud configuration, the oil inlet temperature at the end of wind-down cycle 3 varied between 106 and 109 °F (41 and 43 °C) as shown in Table III. Figure 10 shows windage power loss data versus surface speed for the U configuration. The rate of increase in windage power loss is observed to be greater above approximately 10,000 ft/min (51 m/s). This is in agreement with observations given in Dudley (Ref. 2) and Diab et al. (Ref. 8). For comparison, at 25,000 ft/min (127 m/s), the power loss for the unshrouded meshed spur gear system for wind-down cycle 3 is approximately 20 hp. In contrast, Figure 11 shows gear windage power loss data with a clamshell enclosure configuration (CS). At 25,000 ft/min, the power loss is nearly the same as for the U configuration.

Recall from Table II that the axial and radial clearances for the CS configuration are smaller than those for the U configuration; axial clearance for the CS configuration is 1.5 in. (38 mm) versus 2.3 in. (57.2 mm) for the U configuration, and radial clearance is 0.8 in. (20.8 mm) versus 1.0/2.5 in. (25.4 mm/63.5 mm). Given that previous researchers (Refs. 5 to 10) had shown decreases in power loss with the use of reduced-clearance shrouding, the authors anticipated a significant decrease in windage power loss for the CS configuration. However, the test results showed only a slight decrease in windage power loss, possibly due to the existence of eight drain holes centered along the midspan of the gear tooth width in the clamshell housing (Figure 4). Analyses by Hill et al. (Ref. 7) on shrouded single spur gears with a centered slot show a marked decrease in the effectiveness of the shrouding when compared with the fully shrouded case. Further, single-gear experiments in air by Handschuh and Hurrell (Ref. 6) found that full shrouding results in a greater decrease in windage power loss than shrouding with 1-in. (25.4-mm) oil drain holes. It is reasonable to conclude that the presence of eight drain holes in the clamshell housing contributed to offsetting any shrouding benefit due to decreased axial and radial clearances relative to an unshrouded configuration. A windage power loss test using smooth shrouds at these CS clearances would be needed to confirm this analysis. The CS configuration test results also emphasize the need to consider optimizing existing gearbox drain holes (e.g., number, size, and location) to reduce windage power losses.

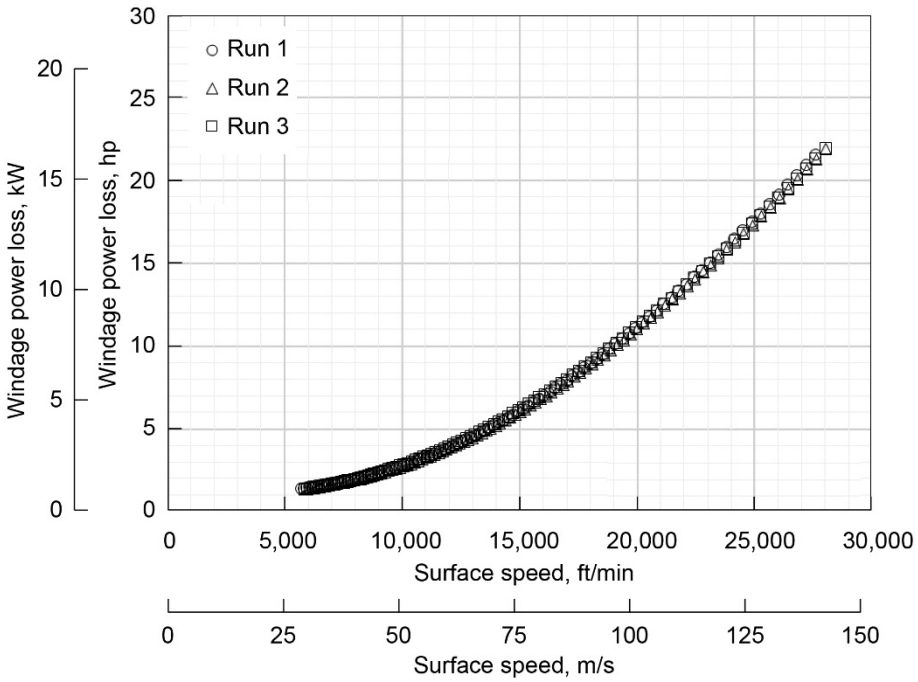

Figure 9.—Repeatability of meshed spur gear windage power loss on three successive test days with shroud configuration C1 (shrouded 0.04-in. (1.00-mm) axial and radial clearance) at a brake torque of 10 in·lb (1.13 N·m). Data included for wind-down cycle 3 only.

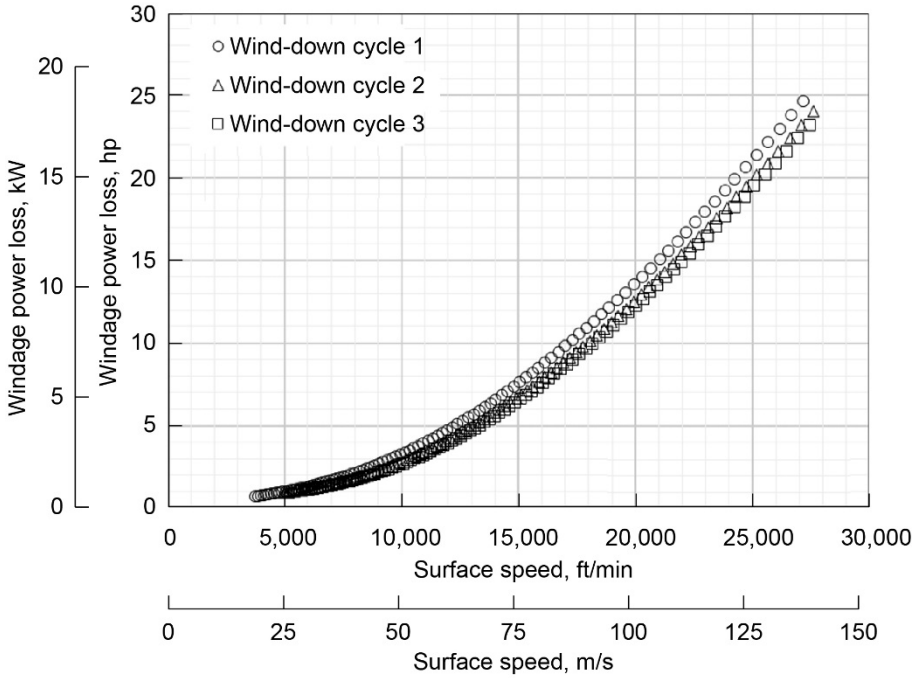

Figure 10.—Meshed spur gear windage power loss for unshrouded (U) configuration at 10-in·lb (1.13-N·m) brake torque.

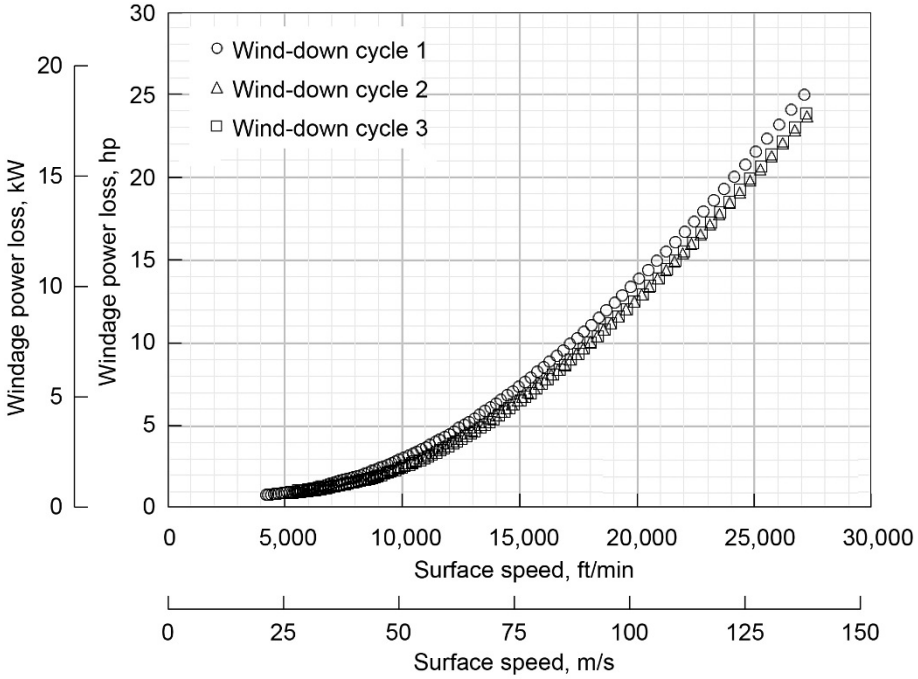

Figure 11.—Meshed spur gear windage power loss for clamshell (CS) configuration at 10-in·lb (1.13-N·m) brake torque.

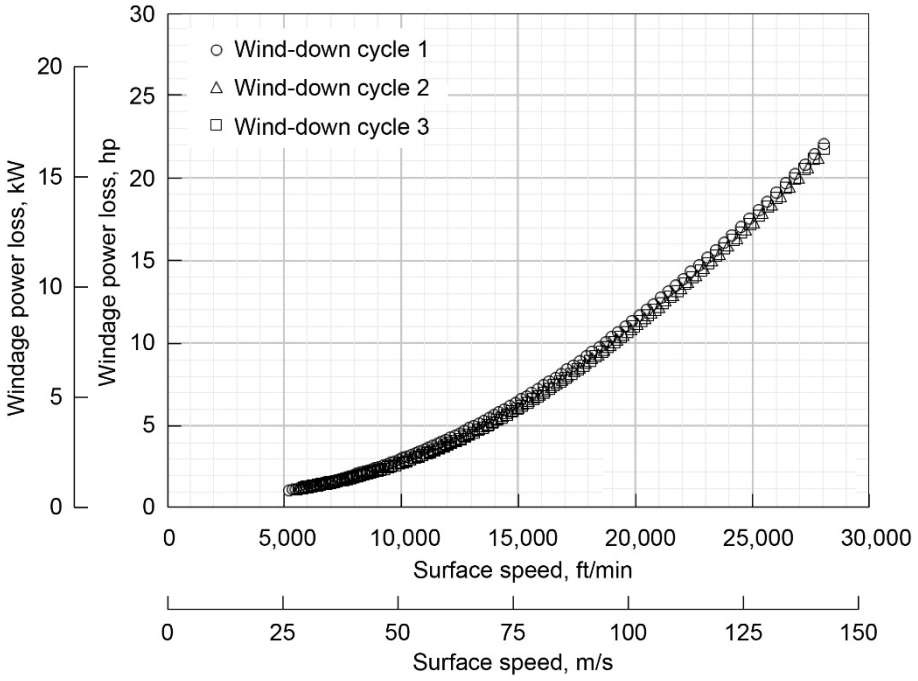

Figure 12.—Meshed spur gear windage power loss for shroud configuration C1 (shrouded 0.04-in. (1.00-mm) axial and radial clearance) at 10-in·lb (1.13-N·m) brake torque.

Figure 12 shows gear windage power loss data for configuration C1 at a clearance of 0.04 in. (1.0 mm) axially and radially. At 25,000 ft/min (127 m/s), the windage power loss is approximately 17.4 hp (13.0 kW), a drop of approximately 10 percent from the unshrouded case. The data for the C1 configuration show how axial and radial shrouding can minimize gear windage power loss. A comparison of shroud

clearances in Table II suggests that close clearances are required for appreciable windage power loss improvements. The effect of axial versus radial clearance changes on power loss will be explored in a subsequent study.

Figure 10 illustrates the effect of increased gearbox oil inlet temperature on gear windage power loss during repeated wind-down cycles. Windage power loss is observed to decrease slightly during each of the three wind-down cycles. For example, at 25,000 ft/min (127 m/s), meshed spur gear windage power losses were 21.0 hp (15.7 kW) for cycle 1, 19.9 hp (14.8 kW) for cycle 2, and 19.4 hp (14.5 kW) for cycle 3. This represents a drop in horsepower of 8 percent between the first and third cycles. As shown in Table III, the oil inlet temperature was observed to increase from 86 °F (30 °C) at the start of wind-down cycle 1 to 101 °F (38 °C) at the end of wind-down cycle 3. Note also that the instantaneous gear fling-off temperature was observed to increase from 165 °F (74 °C) at the start of wind-down cycle 1 to 196 °F (91 °C) at the start of wind-down cycle 3. The gear fling-off temperature is defined as the temperature of the air–oil mixture at the start of wind-down during any of the three wind-down cycles during a test. Increases in internal gearbox temperatures lower the oil viscosity, thereby reducing gear windage drag. This agrees with observations by Lord (Ref. 10). Note that the oil inlet temperature increased by 15 °F (8 °C) and the gear fling-off temperature increased by 31 °F (17 °C) in that same time period. For liquids, viscosity decreases with increasing temperature. For gases, viscosity increases with increasing temperature (Ref. 13). The data on decreasing windage power loss with repeated cycles is suggestive of decreased viscous shear drag due to decreasing fluid viscosity. However, as the gearbox environment is also gaseous (i.e., air), the effect of the air in the gearbox on windage power loss will need to be quantified in a future study. The influence of the gear fling-off temperature and the oil inlet temperature will also be the focus of a future study.

Table IV shows the increase in oil flow for wind-down cycles 1 to 3 for each of the three configurations tested. For the C1 configuration, cycle 3 oil flows are given for Runs 1 and 2 in addition to Run 3 to show repeatability. Increasing oil flow has been observed to increase windage power loss (Ref. 10). Further study is required to determine the extent of that increase. However, the data offer some guidance. First, from Table III it is observed that a variation in gear fling-off and oil temperature of only a few degrees Fahrenheit separates Runs 1 to 3 for the C1 configuration. Next, from Table IV, for the same C1 configuration, it is observed that there is only a 0.037-gal/min (0.140-L/min) difference in oil flow rate for Runs 1 to 3. Finally, nearly identical windage power loss results in Figure 9 for the C1 configuration, Runs 1 to 3, suggest the need to regulate gearbox temperatures and oil flows to control windage power loss. For all configurations tested, comparing oil flows in Table IV with windage power loss data given in Figure 10 to Figure 12 suggests slightly lower values for wind-down cycles 2 and 3 compared with wind-down cycle 1 due to increased oil flow. This potential difference is seen more readily above 10,000 ft/min (51 m/s). This difference may have less of an effect for shrouded configurations such as C1 than for the U and CS configurations.

TABLE III.—SUMMARY OF GEAR FLING-OFF AND OIL INLET TEMPERATURES FOR UNSHROUDED (U), CLAMSHELL (CS), AND SHROUDED (C1) TEST CONFIGURATIONS

Wind-down cycle	Configuration				
	U Run 1	CS Run 1	C1 Run 1	C1 Run 2	C1 Run 3
Instantaneous gear fling-off temperature, °F (°C)					
1	165 (74)	171 (77)	192 (89)	191 (88)	194 (90)
2	184 (84)	187 (86)	208 (98)	206 (97)	210 (99)
3	196 (91)	199 (93)	218 (103)	219 (104)	222 (106)
Oil inlet temperature, °F (°C)					
Start of cycle 1	86 (30)	86 (30)	92 (33)	91 (33)	95 (35)
End of cycle 3	101 (38)	104 (40)	108 (42)	106 (41)	109 (43)

TABLE IV.—SUMMARY OF AVERAGED OIL FLOWS FOR UNSHROUDED (U), CLAMSHELL (CS), AND SHROUDED (C1) TEST CONFIGURATIONS

Wind-down cycle	Configuration				
	U Run 1	CS Run 1	C1 Run 1	C1 Run 2	C1 Run 3
	gal/min (L/min)				
1	0.651 (2.464)	0.676 (2.559)	----------	----------	0.740 (2.801)
2	0.688 (2.604)	0.776 (2.937)	----------	----------	0.813 (3.078)
3	0.753 (2.850)	0.940 (3.558)	0.890 (3.369)	0.873 (3.305)	0.910 (3.445)

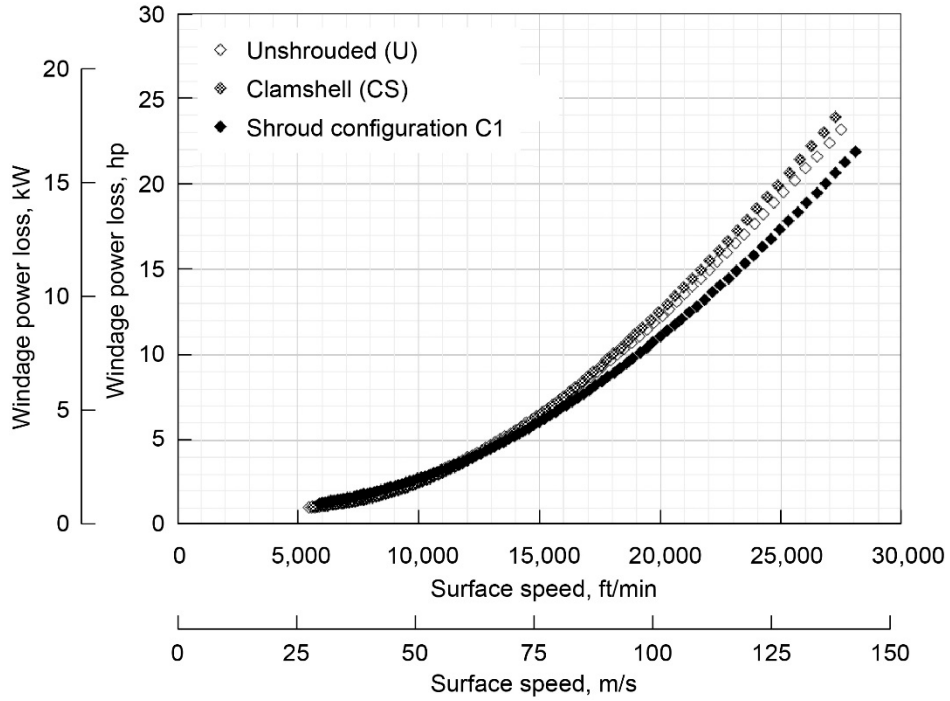

Figure 13.—Comparison of meshed spur gear windage power loss for unshrouded (U), clamshell (CS), and shrouded (C1) configurations at 10-in·lb (1.13-N·m) brake torque.

Shrouding for meshed spur gears is observed to effectively decrease windage power loss above 15,000 ft/min (76 m/s). Figure 13 shows how the power loss data for configurations U and CS versus C1 begin to noticeably diverge above 15,000 ft/min. As noted previously, this supports findings by Dudley (Ref. 2) and Diab et al. (Ref. 8) that windage power loss becomes more significant above 10,000 ft/min (51 m/s). As mentioned by Hill et al. (Ref. 7), this may be due to increasing compressibility effects at speeds approaching Mach 0.3 or roughly 20,000 ft/min (102 m/s) for this specific gear set. Brennen (Ref. 14) shows that the sonic velocity may be lower for two-phase flow (e.g., an air and oil environment). Comparing U versus C1 configurations at a given surface speed, the power loss differential above 15,000 ft/min is observed to increase with surface speed. For example, at 15,000, 20,000, and 25,000 ft/min (127 m/s), the power loss differential is 7, 9, and 10 percent, respectively. Data by Handschuh and Hurrell (Ref. 6) for a single 13-in. (330-mm) pitch diameter spur gear in an air–oil environment with a 1-in. (25-mm) circumferential drain show diverging power loss values through 50,000 ft/min (254 m/s). Further experiments at higher surface speeds are needed to determine if this difference in power loss is relatively constant or if it increases or even decreases.

As noted with the clamshell configuration, the presence of oil drain holes has likely reduced the effectiveness of shrouding in reducing windage power loss. Recall that the C1 shroud configuration shown in Figure 6 has drain holes in both the drive-side and driven-side shrouds. Thus, the maximum decrease in power loss for the meshed spur gear configuration is likely lower than that shown in Figure 13.

Accounting for gear pitch diameter and tooth module (M), where $M = 25.4/P_d$, results from the literature are comparable with results from these studies. Lord (Ref. 10) tested unshrouded meshed spur gears at approximately 2 times into-gear-mesh oil flow. The gears had a diametral pitch, P_d, of 25.4 teeth per inch ($M = 1$), a 75 percent greater tooth width than the NASA gear, and an outer diameter of 8 in. (203 mm). At 21,000 ft/min (107 m/s), the measured windage power loss was approximately 3 hp (2200 kW). This is 4 times less than the NASA unshrouded (U) configuration at the same surface speed (Figure 13). The NASA gear, $P_d = 4$, has an equivalent module of 6.35 (Ref. 15). Experiments by Lord showed an increase in windage power loss with increasing module. For example, increasing the module from 1 to 5 mm (P_d change from 25.4 to 5.08) showed approximately a 5-times increase in windage power loss at 20,500 ft/min (104 m/s) for a 3.5-in. (88.9-mm) diameter spur gear with a face width of 0.47 in. (12 mm). Dawson (Ref. 5) showed similar trends in power loss with increasing module. The effect of gear tooth size on power loss was also observed experimentally by Diab et al. (Ref. 8) and Dawson and then corroborated analytically by Hill et al. (Ref. 7) in that the majority of the windage power losses are due to pressure losses at the gear teeth as opposed to shear effects from a disk of similar size. Note that the experiments (Diab et al. and Dawson) and analyses (Hill et al.) were done with a single gear or disk and in an air-only environment. Single-gear experiments by Handschuh and Hurrell (Ref. 6) with and without lubricant present were inconclusive with respect to power loss trends. Finally, the larger-diameter NASA gears (11.5- and 13.0-in. pitch diameter) (292 and 330 mm) increased windage power loss from viscous drag due to the increased surface area on the sides of the gear.

Comparing a single unshrouded spur gear with meshed unshrouded spur gears, Lord (Ref. 10) comparatively observed that at 21,000 ft/min (107 m/s), unshrouded meshed spur gears showed a power loss increase approximately 3 times that of unshrouded single spur gears, 2.8 hp (2.1 kW) versus 0.87 hp (0.65 kW). For an unshrouded single 13-in. (330-mm) pitch diameter spur gear at 21,000 ft/min, Handschuh and Hurrell (Ref. 6) observed a power loss of 2 hp (1.5 kW). This value is 6.75 times less than that of the tested unshrouded meshed configuration (power loss = 13.5 hp) (10.0 kW) (Figure 13). Clearly, independent observations show a more than doubling of the power loss when testing single versus meshed unshrouded spur gears. The additional drag losses may be partially due to pumping losses, as described experimentally and analytically by a number of researchers (Refs. 16 to 18). Pumping losses are commonly described as the squeezing of the incompressible oil film in the interspatial regions between meshing spur gear teeth. The pumping loss model of Seetharaman and Kahraman (Ref. 18) compares favorably with data given in Figure 13. For a module of 2.32 mm ($P_d = 10.95$) and face width of 1.05 in. (26.7 mm) at 9890 ft/min (50.2 m/s), the predicted power loss is 1.5 hp (1.1 kW). This is 1.75 times less than the unshrouded data in Figure 13 at the same surface speed. As NASA's 6.35-mm gear module is 2.7 times more than the 2.32-mm module of Seetharaman and Kahraman, one would expect an increase in power loss with increasing module. Additional experimental and analytical work is needed to understand how the pumping losses affect total windage power loss.

Comparing shrouded spur gear data, Handschuh and Hurrell (Ref. 6) observed a loss of less than 1 hp (0.7 kW) at approximately 21,000 ft/min (107 m/s) for a single 13-in. (330-mm) pitch diameter gear with a 0.034-in. (0.86-mm) radial shroud clearance and a 0.050-in. (1.27-mm) axial shroud clearance. Additionally, a 1.0-in. (25-mm) rectangular oil drain hole was located at the bottom of the shroud. For a single spur gear ($M = 1$, $P_d = 25.4$), Lord (Ref. 10) observed a power loss of approximately 2.3 hp (1.7 kW) at 21,000 ft/min. Shrouding clearance was 0.04-in. (1-mm) radial and 0.04-in. (1-mm) axial with an oil flow

rate of 0.66 gal/min (2.50 L/min). In comparison, the C1 shrouded configuration with two 4.0- by 0.75-in. (102- by 19-mm) drain holes shows a gear windage power loss of 12.2 hp (9.1 kW) (Figure 13), a value 6 to 12 times that determined by Lord or Handschuh and Hurrell. Possible reasons for the increased windage power loss include use of a NASA gear 30 percent larger in diameter than that used by Lord; a larger equivalent module (M = 6, P_d = 4.2) than Lord's; and possibly complex flows, leading to pumping losses, due to meshed spur gears as opposed to a single rotating gear. Also, a 10 in·lb (1.1 N·m) brake torque was applied during the NASA tests. Previous tests have shown that this adds 0.8 hp (0.6 kW) at 21,000 ft/min.

Concluding Remarks

Gear windage power loss tests were conducted at ambient temperature on meshed spur gears in three configurations: unshrouded (U), clamshell (CS), and shrouded (C1). The results were compared with those found in the literature. The following conclusions are given:

1. The rate of windage power loss was observed to become significant above 10,000 ft/min (51 m/s). This is in agreement with results from the literature.
2. The need for gearbox oil drain slots limits the effectiveness of shrouding in reducing windage power loss.
3. Windage power loss for the C1 configuration was observed to decrease by 10 percent at 25,000 ft/min (127 m/s) compared with the U configuration at the same surface speed.
4. Windage power loss was observed to decrease with increasing oil inlet temperature.
5. Windage power loss was observed to increase with increased oil flow.
6. Shrouding was observed to become more effective above 15,000 ft/min (76 m/s) compared with the unshrouded configuration.
7. Accounting for the effect of tooth module and gear pitch diameter, the unshrouded meshed spur gear power loss results are comparable to the literature.
8. Windage power loss for unshrouded meshed spur gears was observed to be 7 times greater than that previously recorded for unshrouded single spur gears.
9. Windage power loss for shrouded meshed spur gears was observed to be 6 to 12 times greater than that for shrouded single spur gears.

Based on this preliminary study, additional research is recommended in the following areas:

1. Effectiveness of shrouding versus oil drain number, size, shape, and location
2. Effectiveness of shrouding while independently changing both axial and radial clearances
3. Shroud effectiveness at higher surface speeds
4. Sensitivity of windage power loss to oil temperature and oil flow
5. Sources of windage power loss that explain the more than doubling of windage power loss comparing single versus meshed spur gears in both the unshrouded and shrouded configurations

References

1. National Aeronautics and Space Administration: NASA Aeronautics Strategic Implementation Plan. NP–2015–03–1479–HQ, 2015.
2. Dudley, Darle W.: Dudley's Gear Handbook. Dennis P. Townsend, ed., McGraw-Hill, New York, NY, 1991.

3. Eastwick, Carol N.; and Johnson, Graham: Gear Windage: A Review. J. Mech. Des., vol. 130, no. 3, 2008, pp. 034001–034006.
4. Federal Aviation Administration: Helicopter Flying Handbook. FAA–H–8083–21A, 2012.
5. Dawson, P.H.: Windage Loss in Larger High-Speed Gears. Proc. Instn. Mech. Engr., vol. 198A, no. 1, 1984, pp. 51–59.
6. Handschuh, Robert F.; and Hurrell, Michael J.: Initial Experiments of High-Speed Drive System Windage Losses. International Conference on Gears, Munich Germany, 2010.
7. Hill, Matthew, et al.: CFD Analysis of Gear Windage Losses: Validation and Parametric Aerodynamic Studies. J. Fluids Eng., vol. 133, no. 3, 2011, pp. 031103-1–031103-10.
8. Diab, Y., et al.: Windage Losses in High Speed Gears—Preliminary Experimental and Theoretical Results. J. Mech. Des., vol. 126, no. 5, 2004, pp. 903–908.
9. Winfree, Don D.: Reducing Gear Windage Losses From High Speed Gears and Applying These Principles to Actual Running Hardware. DETC2013–13039, 2013.
10. Lord, Andrew Alan: Experimental Investigation of Geometric and Oil Flow Effects on Gear Windage and Meshing Losses. Ph.D. Thesis, Univ. of Wales Swansea, 1998.
11. Anderson, N.E.; and Loewenthal, S.H.: Effect of Geometry and Operating Conditions on Spur Gear System Power Loss. J. Mech. Des., vol. 103, no. 1, 1981, pp. 151–159.
12. Genta, G.; and Delprete, C.: Some Considerations on the Experimental Determination of Moments of Inertia. Meccanica, vol. 29, no. 2, 1994, pp. 125–141.
13. Fox, R.W.; and McDonald, A.T.: Introduction to Fluid Mechanics. John Wiley & Sons, Inc., New York, NY, 1992.
14. Brennen, Christopher E.: Fundamentals of Multiphase Flow. Cambridge University Press, Cambridge, England, 2005.
15. QTC Metric Gears: Elements of Metric Gear Technology. 2017. http://qtcgears.com/tools/catalogs/PDF_Q420/Tech.pdf Accessed Aug. 24, 2017.
16. Pechersky, M.J.; and Wittbrodt, M.J.: An Analysis of Fluid Flow Between Meshing Spur Gear Teeth. Proceedings of the 1989 International Power Transmission and Gearing Conference, vol. 1, Chicago, IL, 1989, pp. 335–342.
17. Diab, Y., et al.: Experimental and Numerical Investigations on the Air-Pumping Phenomenon in High-Speed Spur and Helical Gears. Proc. Inst. Mech. Eng. C J. Mech. Eng. Sci., vol. 219, no. 8, 2005, pp. 785–800.
18. Seetharaman, Satya; and Kahraman, Ahmet: A Windage Power Loss Model for Spur Gear Pairs. Tribol. T., vol. 53, no. 4, 2010, pp. 473–484.